ELSEVIER

Contents lists available at ScienceDirect

Materials Today Sustainability

journal homepage: https://www.journals.elsevier.com/ materials-today-sustainability



Evolution of material properties during the solvent-assisted recycling of thermosetting polymers: to reduce the residual stress and material inhomogeneity



X. Shi ^{a, b}, D. Soule ^a, Q. Ge ^c, H. Lu ^b, K. Yu ^{a, *}

- ^a Department of Mechanical Engineering, University of Colorado Denver, Denver, CO 80217, USA
- b National Key Laboratory of Science and Technology on Advanced Composites in Special Environments, Harbin Institute of Technology, Harbin, 150080, PR China
- ^c Department of Mechanical and Energy Engineering, Southern University of Science and Technology, Shenzhen, 518055, China

ARTICLE INFO

Article history: Received 10 August 2021 Received in revised form 20 February 2022 Accepted 15 May 2022 Available online 26 May 2022

Keywords: Transesterification Bond exchange reactions Anhydride epoxy Thermoset recycling Mechanical properties

ABSTRACT

Primary recycling of thermosetting polymers is shown to be enabled by depolymerizing the material in a suitable organic solvent and then re-polymerizing it into near-identical networks with equivalent mechanical properties. The re-polymerization process involves sophisticated coupling among solvent diffusion, chemical reaction, and stress field development. Specifically, solvent evaporation leads to restrained volume shrinkage of the resin and residual stress development within the re-polymerized materials. Nonuniform curing degree and material properties are also developed in the direction of solvent diffusion. These impose grand challenges to identify the optimal processing conditions to recycle thermosets with high quality and high speed. In this paper, using an integrated experimental and theoretical approach, the evolutions of the stress field and material properties during the repolymerization of thermosetting polymers are studied. It shows how to tune the processing temperature to mitigate the residual stress and material inhomogeneity of recycled thermosets. The influencing mechanisms of sample thickness and catalyst content are also revealed. The fundamental understanding is finally extended to study the manufacturing of composites with particle reinforcements using the depolymerized solution, with a particular emphasis on the minimization of the stress concentration around particles. Overall, this study provides a guideline to design material and processing conditions for homogeneous network structure and mechanical properties of recycled thermosets, which will promote the applications of the green recycling method for thermoset wastes and benefit society.

© 2022 Elsevier Ltd. All rights reserved.

1. Introduction

Thermosetting polymers are covalently cross-linked networks with excellent mechanical strength, thermal stability, and chemical resistance [1]. They are irreplaceable in many high-performance engineering applications such as ground transportation and aerospace engineering. However, due to their permanently cross-linked networks, they are extremely hard to reprocess and recycle using conventional methods, leading to ever-increasing contaminations in the waterways, wildlife, and human bodies.

A wide variety of processing techniques have been developed to reuse or recycle thermoset wastes. For example, mechanical

* Corresponding author. E-mail address: kai.2.yu@ucdenver.edu (K. Yu). recycling [2–7] involves shredding or milling of the scraps into powder to be reused as additives in other applications. Thermochemical recycling methods, such as pyrolysis and solvolysis [8–14], use high temperature, pressure, or supercritical chemicals to decompose the network. They can be applied to reclaim valuable reinforcements (e.g., carbon fiber) in the thermoset matrix, but the harsh processing conditions are inconvenient to handle and economically unfavorable for industrial applications. In addition, the decomposition products are a complicated mixture of gaseous, liquid, and solid chemicals, which are hard to be reused and may become secondary contamination.

Benefited from the recent development of dynamic chemistry, innovative recycling methods using organic reactive solvents have been developed, wherein the solvent molecules diffuse into the network and break the polymer chains at target covalent bonds.

With sufficient solvent provided, the network will be gradually degraded into oligomer liquid. As a notable example, Wang et al. [15] showed that an amine-cured epoxy, which is widely used in aerospace engineering, could be decomposed in AlCl₃/acetic acid solution at 180 °C. Some commercial curing agents are designed to recycle thermosets in a similar principle. Connora Tech. Inc. (Hayward, CA) commercialized a dynamic epoxy cross-linker, Recyclamine®, which enables the network to depolymerize in acetic acid at 80 °C [16] due to the selective cleavage of cross-linking sites. Since the main skeleton of the polymer chain is preserved, the depolymerized oligomer can be reused as thermoplastics or cross-linked with other monomers. A comprehensive review of the recycling methods based on dynamic bonds can be found by Ma et al. [17].

Depending on the employed dynamic chemistry, the decomposition process can be fully reversible, namely, the cleaved bonds can be reconnected to enable the primary recycling of thermosets. One prominent example is to utilize the bond exchange reactions (BERs) [18–29]. For example, Yu and coworkers demonstrated that a thermosetting epoxy with transesterification BERs can be depolymerized in ethylene glycol (EG) due to the BERs between ester bonds on the chain backbone and EG molecules [30-36]. The depolymerization product can be re-polymerized into a new polymer with near-identical mechanical properties as unprocessed polymers. Similarly, thermosets with dynamic disulfide bonds were shown to be recycled using thiol-containing solvents [36,37]. Thermosetting polyimine with dynamic imine BERs were shown to be recycled using diamine solvents [38–43]. In general, the solventassisted recycling of thermosets involves simple heating in a proper organic solvent to realize primary recycling at mild processing conditions. It shows great potential to ease environmental and economic concerns associated with the traditional disposal techniques and meet the pressing demand for polymer recycling.

To promote the immediate applications of the recycling method and benefit society, a complete understanding of the material-process-property relationship is required. For example, how do the material properties evolve during the recycling, and how do they relate to the temperature and other processing parameters? Answer to these questions can assist the design of optimal processing conditions to improve the quality of recycled thermosets, as well as to reduce the processing cost and environmental burden. In our recent work [44], a multiscale chemomechanics modeling framework was developed that directly links the microscale network structure to the macroscale material properties. At the macromolecular level, the chemical reaction rates were formulated to determine the average chain segment length and network degree of curing (DoC). The evolution rule of DoC was then fed into the continuum-level mechanics model to effectively capture the evolution of thermoset thermomechanical properties during the re-polymerization.

To gain a fundamental understanding of the recycling method, the previous work [44] focused on the re-polymerization process of thin-film thermosets, wherein the distribution of solvent molecules and material properties were relatively uniform. The repolymerization process was also assumed to be in a free-standing state without stress. However, these are the ideal processing conditions that cannot be met in practical applications of the recycling method. First, due to the restrained volume shrinkage of polymer resins in a mold, the solvent evaporation will lead to notable residual stress development. This could a major concern when preparing composite materials using the depolymerized polymer solution, which may lead to the shape distortion or material failure of the recycled thermosets. Second, re-polymerization of the thermoset starts from the surface as the solvent evaporates. Nonuniform solvent content, conversion of functional groups, and network

structure will be developed in the thickness direction. This imposes challenges to identify the optimal processing temperature for recycling. For example, a higher temperature will lead to a stiff film quickly formed on the solution surface, but it will suppress the solvent evaporation, and consequently the re-polymerization of materials beneath it. While a lower temperature leads to relatively uniform material properties evolution, the trade-off will be the low reaction rate and recycling speed. These phenomena deserve rigorous study before the recycling techniques can be widely adopted in practical applications.

In this paper, the evolution of residual stress and distribution of material properties during the re-polymerization of bulk thermosets are studied. An epoxy-based thermosetting polymer is used as the material platform. The influences of heating temperature are experimentally investigated. A diffusion—reaction—kinetic modeling framework is then developed to capture the experimental observation and assist the discussion. With the solvent-evaporation boundary condition, the transportation of solvent molecule and the distribution of DoC along the sample thickness direction is formulated, which determines the evolution of network residual stress and mechanical properties using a continuum-level mechanics model. It is applied to perform parametric studies to examine the influences of BER catalyst content, material thickness, and curing temperature on the re-polymerization speed. Finally, the evolution of residual stress during the composite manufacturing with particle reinforcements is investigated. The presented study advances the understanding of the structural-processing-property relationships during the recycling of thermosets and their composites. It also reveals the influencing mechanisms of various material and processing conditions, which provides a guideline to design material and processing conditions for homogeneous network structure and mechanical properties of recycled thermosets.

2. Materials and methods

2.1. Material synthesis

The epoxy sample used in this study is an epoxy-based thermoset developed by Leibler and coworkers [45], which can perform transesterification BERs at high temperatures (e.g., >120 °C). They were synthesized from a mixture of dimers and trimers of fatty acids (Pripol 1040, Croda, Houston, TX), monomers diglycidyl ether of bisphenol A (DGEBA, Sigma Aldrich, St. Louis, MO), and a metal catalyst Zn (Ac)₂ for transesterification BERs (Sigma Aldrich). Detailed chemical structures of each reagent are shown in Fig. 1.

During the polymer synthesis, the catalyst was first mixed with the fatty acid (10 mol% to COOH groups) in a round-bottom beaker. The temperature was gradually increased from 100 °C to 150 °C while maintaining the mixture under vacuum. After being heated for ~3 h, no gas evaporation was observed, and the catalyst particles were completely decomposed, suggesting that the fatty acids fully replaced the acetates as ligands of Zn. Subsequently, the monomer DGEBA was added to the mixture, wherein the stoichiometry ratio between COOH and epoxy was 1:1. The mixture was manually stirred until homogeneous. Finally, the mixture was poured into a mold. The network was fully polymerized after heating in an oven for 6 h at 160 °C.

2.2. Preparation of the depolymerized polymer solution

The synthesized epoxy network contains ester bonds on the chain backbone and catalyst for transesterification BERs. When the sample is immersed in the EG solvent, the hydroxyl groups of the diffused solvent molecules will participate in BERs with the ester

CH₃ CH₃

$$CH_3$$

CH₃
 CH_3
 CH_3

Fig. 1. Chemical structures of the chemical reagents used in this study.

bonds and break the chains on the backbone (Fig. 2), which eventually depolymerize the network into a liquid oligomer.

The as-fabricated epoxy samples were immersed in EG solvent at 180 °C for network decomposition. An excessive amount of solvent was used to make sure the network was fully depolymerized into soluble chain segments. The volume ratio between the polymer and solvent was 0.6:1. The depolymerization speed depended on the temperature. For example, a 5 cm cubic sample was shown to be fully depolymerized after being heated at 180 °C for ~6 h. During the heating, the container was sealed to avoid solvent evaporation. After the sample was fully decomposed, there are unreacted solvent molecules in the mixture. Since the mole amount of reacted EG molecules equaled to the ester bonds on the chain backbone, the amount of unreacted EF molecules in the mixture was known.

For the re-polymerization, the depolymerized polymer solution was poured into a mold and placed in an oven for heating in an open environment. The sample thickness changed for different types of tests, which will be introduced in the following sections. During the heating, the network gradually polymerized as the solvent evaporated out of the system (Fig. 2). The heating time and temperature were varied during the tests to examine their influences.

2.3. Residual stress measurements during the re-polymerization

Volume-shrinkage-induced residual stress is a major concern during the fabrication of thermosets and their composites. When preparing thermosets in a confined environment using the decomposed polymer solution, the residual stress development could be notable due to the significant volume shrinkage resulted from the evaporation of solvent molecules.

To characterize the development of residual stress in the repolymerizing network, the polymer solution was poured into a mold with 1.5 mm thickness and was heated at 180 °C in an open environment. After being heated for 50 min, the sample passed the gelation point and could carry the load. The sample thickness at this point was approximately 0.8 mm. The samples were then transferred to the dynamic mechanical analysis (DMA, Model Q800, TA Instruments, New Castle, DE, USA), wherein the length was fixed during the isothermal heating process at different temperatures. The stress increment of the network due to volume shrinkage was recorded.

2.4. Measurements of solvent diffusivity with different epoxy curing degree

The re-polymerization of bulk epoxy sample is a diffusion—reaction—mechanics problem, wherein the network curing starts from the sample surface, and the solvent molecules diffuse toward the top curing layers. Therefore, it is important to determine the solvent diffusivity within epoxy networks with different curing degrees.

To prepare the epoxy samples, the precursor resin containing DGEBA, fatty acid, and catalyst (as described in Section 2.1) was poured into a mold with a thickness of 1.5 mm. After heating the resin at 130 °C for different times, the samples were taken out and subject to DMA (Model Q800, TA Instruments, New Castle, DE, USA) to determine the network glass transition temperature (T_g). The tests were performed at a frequency of 1 Hz, and the temperature

Fig. 2. Schematic representation of the cleavage and reconnection of polymer chains during the network depolymerization and re-polymerization.

was increased from -30 °C to 100 °C at a rate of 2 °C/min. As will be introduced in the Constitutive Modeling section, the network T_g can be directly scaled to the curing degree. A higher T_g suggests a higher DoC value and network cross-linking density.

The epoxy samples with different curing degrees were then subject to swelling tests to identify the diffusivity of EG solvent. The samples were cut into the identical dimension (10 mm \times 10 mm \times 1.5 mm) and immersed in 10 g EG solvent in a flask at 100 °C. Not BER catalyst was added into the solvent, so the samples kept swelling without depolymerization. The mass increment of the samples was recorded to calculate the solvent diffusivity.

2.5. Thermomechanical properties of the nonuniform repolymerizing network

To characterize the nonuniform material properties during the re-polymerization of bulk epoxy, the depolymerized polymer solution described in Section 2.2 was poured into a mold with a 20 mm depth. After being heated at a specific temperature for a given time, the sample was taken out and sliced into layers parallel to the thickness direction of the sample, as shown in Fig. 3. It is important to note that, during the re-polymerization, the sample thickness decreased notably with the solvent evaporation. After the network was fully polymerized, the thickness was reduced to ~7 mm. However, when the sample was sliced, the thickness of each layer was set to be ~1.5 mm in all cases, which was small enough to assume relatively uniform material properties in each layer. The sliced samples were then subject to DMA tests to examine their thermomechanical properties, including the storage modulus and network T_g . During the DMA experiments, the samples were first stabilized at -30 °C for 10 min to reach the thermal equilibrium. Then, the strain oscillated at a frequency of 1 Hz and the temperature was increased from -30 °C to 100 °C at a rate of 2 °C/min.

3. Constitutive modeling

3.1. Overview of the modeling framework

The overall modeling framework is shown in Fig. 4. The repolymerization of bulk epoxy sample is taken to be a 1D diffusion—reaction—mechanics problem with solvent evaporation boundary condition applied on the top surface (x = 0), which drives the diffusion of solvent molecules in the vertical direction of the system. With the decreasing amount of solvent molecules, the equilibrium of the reversible reactions in Fig. 2 will shift toward the direction of chain connection, which increases the network curing degree. From the bottom to the surface of the system, the network

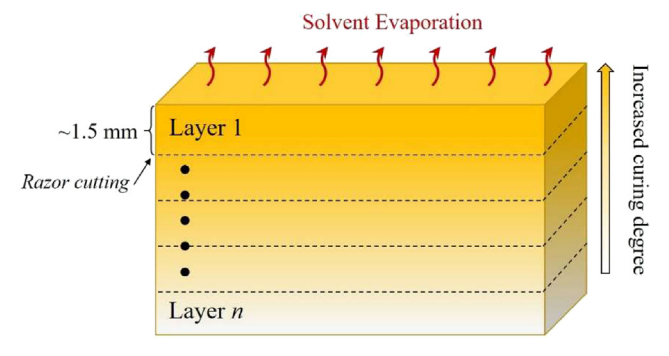


Fig. 3. Schematic illustration of the layering of bulk materials.

has a decreasing solvent content and an increasing curing degree. For a specific layer at x, the chain cleavage and reconnection rates depend on the content of solvent molecules, as well as the content and length distribution of chain segments. These quantities determine the DoC of the local network, which further scales to the network volume shrinkage, amplitude of residual stress, and thermomechanical properties.

For the solvent—evaporation boundary condition, an exponential equation is adopted to describe the relationship between the evaporation rate r_0 (mass loss per second and unit area) and temperature T:

$$r_0 = a_1 \exp(a_2 T), \tag{1}$$

where a_1 and a_2 are two fitting parameters determined by experimental data.

The transportation of solvent within the system is assumed to follow Fick's second law. The mole content of solvent molecule $C_{eg}(x,t)$ is formulated by:

$$\frac{\partial C_{eg}(x,t)}{\partial t} = D_s(x,t) \frac{\partial^2 C_{eg}(x,t)}{\partial x^2} + k(x,t), \tag{2}$$

where D_s denotes the solvent diffusivity, and k denotes the changing rate due to the transesterification BERs. Both parameters depend on the network curing degree (*i.e.*, cross-linking density) and thus are functions of layer position and heating time. The temperature dependence of D_s follows the Arrhenius law. According to Krongauz et al. [46], the solvent diffusivity is scaled with the network cross-linking density by an exponential relationship. With these considerations, the D_s is formulated as

$$D_s = D_{s0} \exp[\alpha(1 - P(x, t))], \tag{3a}$$

where

$$D_{s0} = D_0 \exp \left[-\frac{E_a}{R(T + 273)} \right]. \tag{3b}$$

In the above equation, α is a scaling factor determined by experimental data. P(x,t) is the DoC $(0 \le P \le 1)$, which depends on the reaction kinetics and will be introduced in detail in the following section. D_{s0} represents the temperature dependency of D_s , with D_0 being a reference diffusivity, E_a being the energy barrier, and R being the gas constant.

According to the previous work [44], the network equilibrium modulus (E_{eq}), which scales to the network curing degree, follows:

$$E_{eq}(x,t) = E_{\infty} P^{6\beta}(x,t), \tag{4}$$

where β is a correlation exponent, and E_{∞} is the equilibrium modulus of a fully cured network.

The network transition temperature is another important indicator of the extent of curing. Following the previous work by Gan et al. [47], the T_g evolution during the re-polymerization is formulated using the empirical Dibenedetto equation [48,49]:

$$T_g = \frac{E_r}{R \ln \left[g_1 (1 - P)^{\xi} + g_2 \right]},\tag{5}$$

where $E_{\rm r}$ is the activation energy of transition from the glassy to the rubbery state, R is the gas constant, and ξ is the parameter for accounting the effects of chain entanglement. g_1 and g_2 are two material constants.

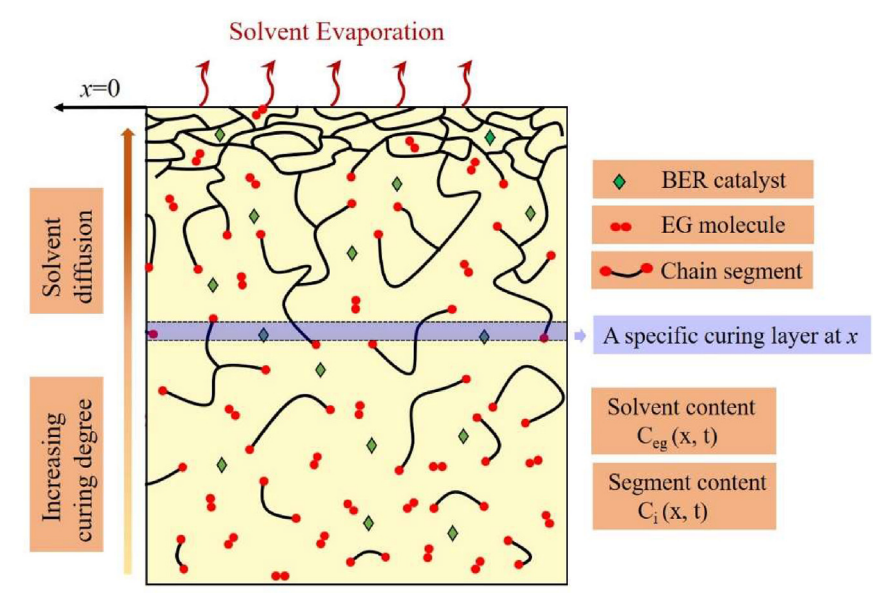


Fig. 4. Overview of the modeling framework for the diffusion—reaction—mechanics problem.

3.2. Microscale reaction kinetics and degree of curing

The network curing degree, P(x,t), can be formulated by considering the microscale reactions of chain cleavage and connection. At a specific position of curing layer, x, the rates of chain connection (k_1) and cleavage (k_2) during the re-polymerization are formulated based on the diffusivity of solvent molecules and chain segments as well as their contents and average distance.

For the chain connection, the chain segments first diffuse toward another reactive site and then connect via BER. The reaction rate k_1 (mol/s) for the chain connection (k_1) can be written as:

$$k_1 = (N_A t_1 + N_A t_{BER})^{-1},$$
 (6a)

where N_A is the Avogadro's number $(6.02 \times 10^{23} \text{ mol}^{-1})$, and t_1 is the traveling time of a segment with i monomers to meet another reactive site at segment tails. Following our previous work, $t_1 = \tau_i (C_r N_A b^3)^{-4/3}$, with τ_i being the Rouse time of the segment i monomers, C_r being the concentration of exchangeable bonds at the segment tails at a continuum point, and b being the monomer length. t_{BER} is average time spent on a BER. $t_{BER} = t_{0_BER} exp(E_{ab}/RT)$, with E_{ab} being the BER energy barrier, and t_{0_BER} being a time constant.

For the chain cleavage reaction, the solvent molecules first diffuse toward an ester bond on the chain backbone and then break the chain via BER. The reaction rate k_1 (mol/s) for the chain can be written as:

$$k_2 = (N_A t_2 + N_A t_{BER})^{-1},$$
 (6b)

where t_2 is the traveling time of the solvent molecule. $t_2 = \langle r_2 \rangle^2 / D_s$, with $\langle r_2 \rangle$ being the average distance between an ester and solvent molecule. According to the theory of mean inter-particle distance, $\langle r_2 \rangle = \frac{1}{3} \Gamma(\frac{1}{3}) a$, where Γ is the gamma function. $a = \sqrt[3]{4N_A \pi C_{ea}/3}$ is the Wigner–Seitz radius.

The rate constants are then used in first-order reaction equations to formulate the content and length distribution of chain segments during the re-polymerization. During the re-polymerization, there are four types of BERs that will change the content of the segment with i monomers (i.e., C_i). As illustrated in Fig. S1 (Supplementary Materials), the four reactions are as follows: (a) a segment with i monomers reacts with an EG molecule and

breaks into two shorter segments; (b) a segment with i monomers reacts with another chain segment to form a longer chain segment and generate a new EG molecule; (c) two short chain segments react to form a segment with i monomers and generate a new EG molecule; (d) a long chain segment react with an EG to form a segment with i monomers and another chain segment. At time t of re-polymerization, the changing rate of C_i is the summation of the reaction rates of the four reactions:

$$\dot{C}_{i} = \underbrace{-k_{2}C_{i} - k_{1}C_{i}}_{r_{i}^{a}} + k_{1} \sum_{j=1}^{i-1} C_{j} \left(C_{i-j} / \sum_{m} C_{m} \right)_{r_{i}^{c}} + k_{2} \sum_{j=i+1} C_{j} \left(2 / \left(j - 1 \right) \right)_{r_{i}^{d}}.$$

$$(7)$$

Solving the above differential equations will determine the content and length distribution of chain segments, as well as the content of solvent molecules. The DoC is defined to be the amount of ester groups on the segment backbone, $\sum_{i=2}^{n} (i-1)C_i(t)$, normal-

ized by its final value in the fully polymerized network:

$$P(t) = \frac{N\sum_{i=2}(i-1)C_i(t)}{(N-1)C_1(t=0)}.$$
(8)

The reaction rates of four possible reactions in Fig. S1 also determine the changing rate of solvent content (C_{eq}) at a material point mentioned in Eq. (2):

$$k(x,t) = \sum_{i=1} \left(r_i^a - r_i^b + r_i^c - r_i^d \right), \tag{9}$$

3.3. Network residual stress development and thermomechanical properties

The development of residual stress is formulated by considering the restrained volume shrinkage during the network repolymerization. Following the previous work [50], the volume shrinkage of the curing network in the free-standing state

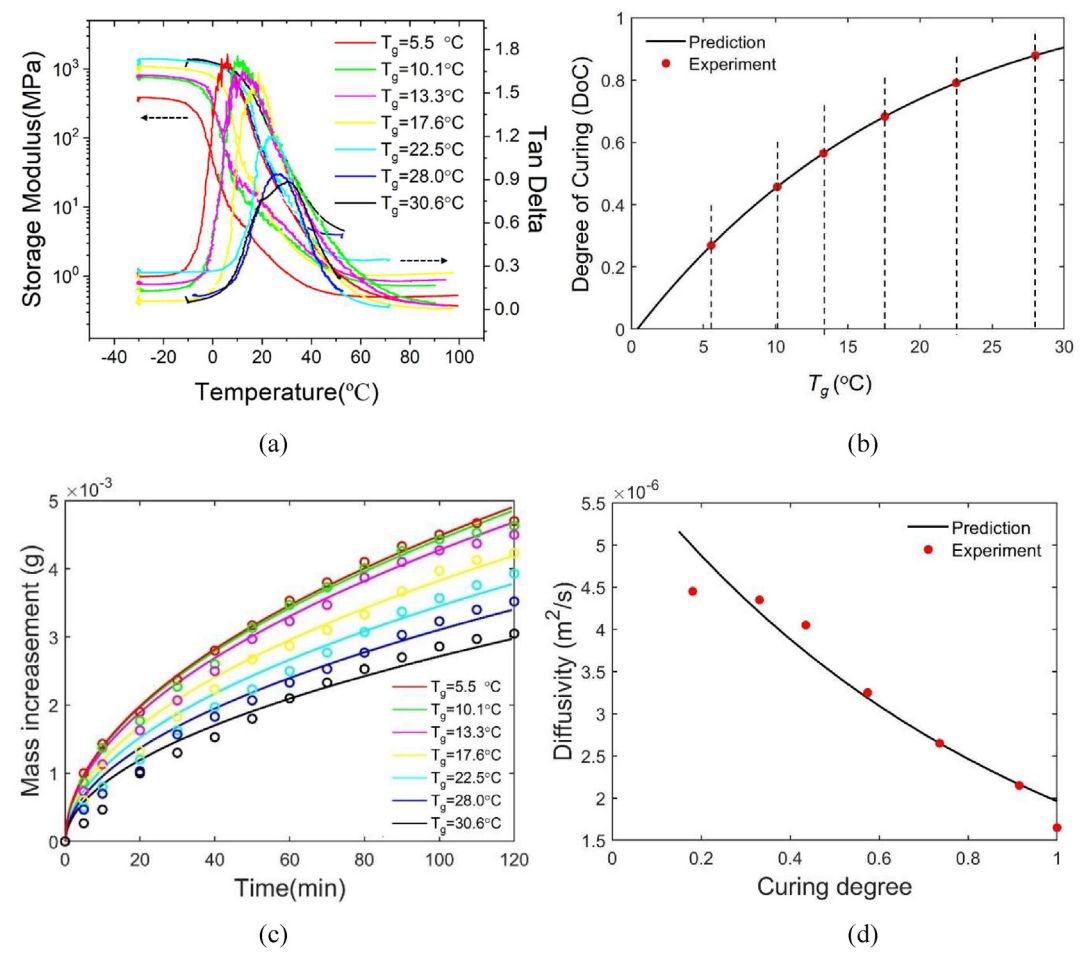


Fig. 5. (a) The T_g of epoxy during the re-polymerization. (b)The evolution of curing degree with T_g during re-polymerization. (c) The mass increment of epoxy with different T_g during swelling test. (d) The diffusivity of solvent in the epoxy network at different curing degree.

is assumed to be in a linear relationship with DoC, namely $\Lambda=(V_0-V)/(V_0)=\chi P$, with χ being a fitting parameter. The stretch ratio of the thermal component is written as: $\lambda_T=\sqrt[3]{1-\chi P}$. With a restrained volume shrinkage condition, stress will be developed within the network during the re-polymerization. However, the evolution of material properties should be considered during the formulation of stress evolution. First, after the network passing the gelation point, the increase of chain segment length leads to a continuous increment in the network cross-linking density and equilibrium modulus E_{eq} . Second, the new network fractions start to carry loads after they are born at different stages of the repolymerization process. They have different reference configurations. Therefore, the residual stress, σ_R evolves with the equilibrium modulus in a time—convolution manner:

$$\sigma_r = \int_0^t \dot{E}_{eq}(s) ln[\lambda_T(t-s)] ds \tag{10}$$

4. Results and discussions

4.1. Material parameters identification

All the material parameters can be determined by standard polymer tests. For example, in our previous work [44], the

parameters of solvent evaporation rate (Eq. (1)) were determined by measuring the mass loss of pure EG solvent at different temperatures. The network cross-linking density of the cured epoxy sample was determined by the network equilibrium modulus (3.2 MPa) obtained from the DMA tests. The density of the mechanically effective chains was determined to be 327.7 mol/m³ based on its relationship with equilibrium modulus and the Boltzmann constant. If we assume the functionality of the crosslinker is four, the network cross-linking density can be estimated to be 163.8 mol/m³. To determine the diffusivity parameters in Eq. (3b), epoxy samples without the BER catalyst were soaked in the EG solvent at different temperatures. At times, their weight was measured to determine the solvent diffusivity. Note that since the sample mass was tracked during the swelling measurements, the amount of solvent diffused into the network-free volume before notable volume expansion was accounted for during the diffusivity characterization.

By measuring the glass transition behaviors of thin-film epoxy samples at different stages of re-polymerization, parameters for the evolution of equilibrium modulus (Eq. (4)) and T_g (Eq. (5)) were determined. The BER activation energy E_{ab} was measured by performing a series of stress relaxation tests on the as-fabricated epoxy samples to determine the relaxation times at different temperatures [51–54]. Finally, the parameter χ characterizing the volume shrinkage (Eq. (10)) was determined by measuring the length shrinkage of a free-standing thin-film sample at high temperatures.

All the material parameters are listed in Table S1 in the Supplementary Materials.

These sets of parameters are shown to be effective to study the re-polymerization of thin-film samples with uniform material properties. When it comes to the re-polymerization of bulk epoxy, it is important to determine the diffusivity of solvent in the network with varying curing degrees. To characterize it, a thin-film epoxy sample was heated for different times, and their glass transition behaviors are shown in Fig. 5a. It is observed that both network T_g and equilibrium modulus increase with the heating time, suggesting a gradually increased network curing degree. With 22 h of heating at 130 °C, the network T_g reaches 30.6 °C, which is close to that of the fresh epoxy sample. Using Eq. (7) with predetermined parameters, the corresponding DoC values of each epoxy sample can be calculated, which are summarized in Fig. 5b.

The epoxy samples with different curing degrees are subject to swelling tests in EG solvent at 100 °C to determine the solvent diffusivity. The dots in Fig. 5c show the experimental results of the mass increment as a function of swelling time. It is observed that the mass increment is faster in the network with a lower curing degree (or cross-linking density), which results from the higher free volume within the network for solvent transportation. For each swelling curve, it is fitted with a diffusion function to calculate the corresponding diffusivity (sold lines in the figure). The determined diffusivities are plotted in Fig. 5d as a function of network DoC. Within the constitutive modeling framework, the relationship between the solvent diffusivity and network DoC follows an exponential relationship (Eq. (3a)). By fitting with the experimental data, the parameter is determined to be $\alpha = 1.137$.

4.2. Evolution of residual stress during the re-polymerization of thin-film sample

There are two mechanisms leading to the network volume shrinkage during the re-polymerization, namely (i) the transition of weak Van-der-Waals interactions among chain segments into covalent bonding and (ii) the solvent evaporation. Considering the significant amount of solvent involved in the process, the second mechanism dominates. The restrained shrinkage of polymer resins leads to notable residual stress during the re-polymerization process.

The experimentally measured residual stress is plotted as a function of heating times in Fig. 6. Note that the sample thickness is

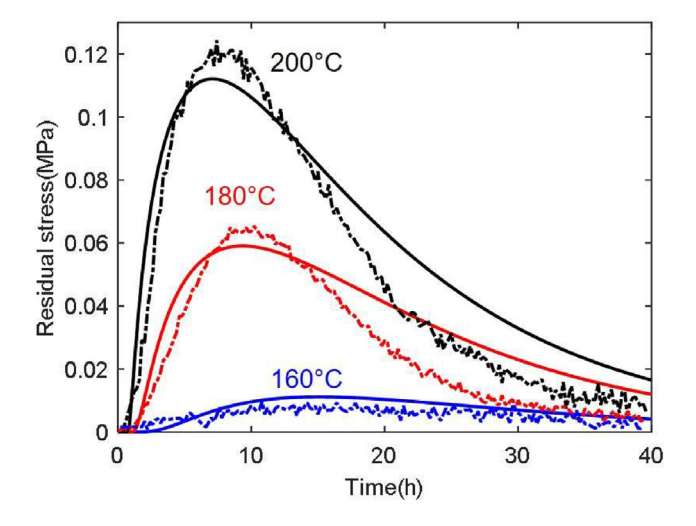


Fig. 6. The evolution of residual stress during the re-polymerization of thin-film epoxy sample. Solid lines: model predictions; dashed lines: experimental data.

less than 1 mm, so it is safe to assume relatively uniform material properties and stress distribution within the network. It is seen that at the early stage of re-polymerization, the residual stress increases due to solvent evaporation and network shrinkage. The increment is almost linear as a function of heating time at different temperatures. However, since the transesterification catalyst does not evaporate, the network can perform transesterification BERs, which effectively release the internal stress. Therefore, the internal stress starts to decrease after reaching the peak value. This phenomenon suggests that the connection of short chain segments during the network re-polymerization is a faster mechanism than the bond exchanging among macromolecular polymer chains for stress relaxation.

Although the internal stress can be eventually released in the epoxy network, the peak stress during the re-polymerization could be a major concern to fabricate high-quality thermoset products. For example, when the heating temperature is 200 °C, the peak stress is shown to be up to ~0.12 MPa. A higher temperature will lead to faster volume shrinkage of the network and thus a higher peak of residual stress, which will result in the sample failure with restrained volume shrinkage conditions, especially when the temperature is highly above the network T_g and the material is brittle. On the other hand, when the temperature is relatively low, the residual stress generated in the system is slow and can be easily released by BERs.

The solid lines in Fig. 6 represent the predictions of the modeling framework. The close comparison with the experimental data shows that the developed model can precisely capture the evolution of the residual stress and peak stress during the repolymerization at different temperatures.

4.3. Evolution of material properties during the re-polymerization of the bulk sample

The evolution of thermomechanical properties of the bulk epoxy samples during the re-polymerization process was studied. Herein, the network T_g and equilibrium modulus E_{eq} (namely the modulus highly above the T_g) were used as the indicators to characterize the curing degree. The evolutions of T_g and E_{eq} of the first four curing layers close to the top surface are plotted in Fig. 7, wherein the curing temperature is 180 °C and 200 °C, respectively. In the figure, the experimental data are plotted as dots and the model predictions are plotted as solid lines. The close comparison suggests that the developed constitutive modeling framework is efficient to capture the nonuniform distribution of material properties during the re-polymerization of the bulk epoxy samples.

From the figure, it is observed that the increments of both parameters are slow at the early stage of re-polymerization, which results from the excessive solvent molecules in the gel-like network suppressing the chain connection reaction. After most isolated solvent molecules are evaporated out of the system, the chain segments start to rapidly connect, and the network T_g and E_{eq} dramatically increase with heating time. The first curing layer, which is essentially on the top surface of the epoxy sample, polymerizes first. With a sufficient heating time (e.g., ~25 h at 180 °C and 17 h at 200 $^{\circ}$ C), the T_g of the first curing layer reaches the same level as the unprocessed sample. The increment of equilibrium modulus is seen to be slower, which might because of some excessive EG molecules left in the network, serving as the chain extender to reduce the cross-linking density. Increasing temperature from 180 °C to 200 °C increases the curing speed of each curing layer, but the delay in the re-polymerization between the first and the rest curing layers tends to be more notable. This is because after a stiff curing layer quickly formed on the surface, it

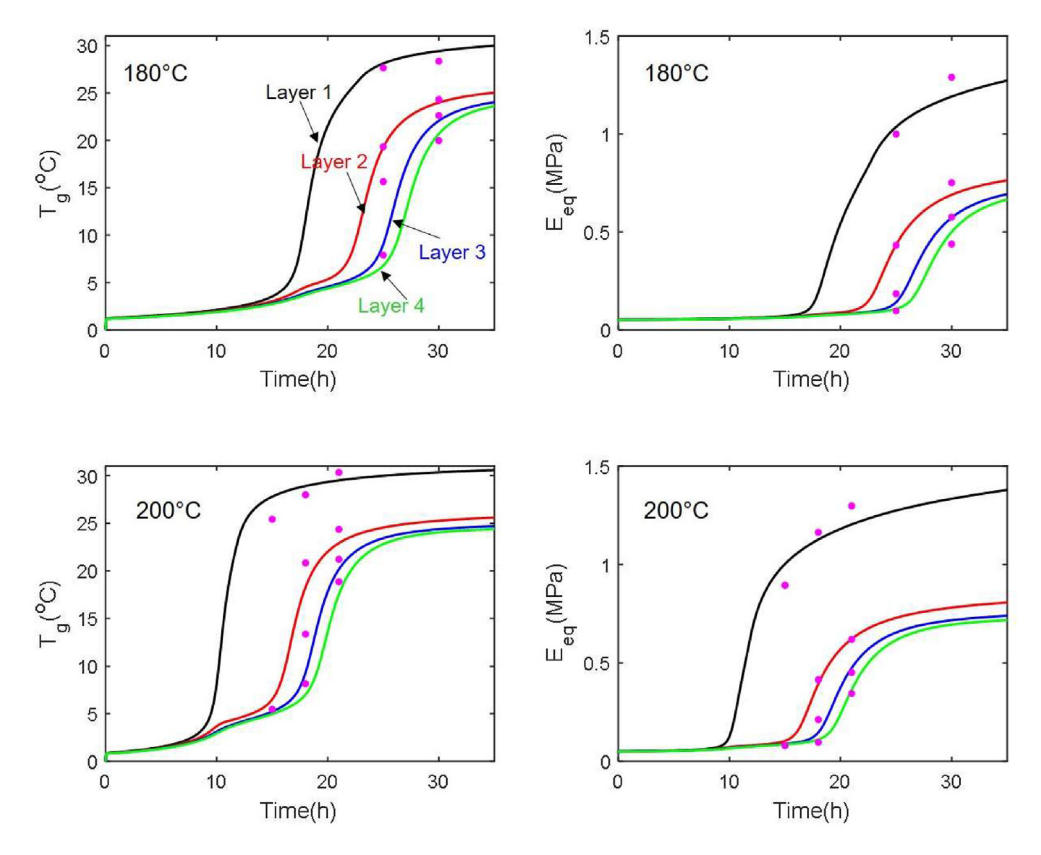


Fig. 7. The evolution of network T_g and equilibrium modulus of the first four curing layers during the re-polymerization of bulk epoxy.

will block the transportation of the solvent modules due to the lower solvent diffusivity and thus suppress the curing of the bottom materials.

4.4. Influences of processing conditions on the re-polymerization speed of the bulk sample

With an effective modeling framework, parametric studies are performed to uncover the relationships between material properties, processing conditions, residual stress, and recycling speed of bulk epoxy.

As shown in Fig. 8a, the evolution of the residual stress in the first four curing layers of the bulk epoxy is predicted at temperatures ranging from 150 °C to 250 °C. The corresponding evolution of DoC of each layer at the same temperatures is plotted in Fig. 8b. It is seen for each testing temperature, after the excessive solvent molecules are evaporated out of the system, both residual stress and DoC value start to dramatically increase at about the same time point. The increment, especially for the first curing layer, is earlier when the curing temperature is higher. For example, when the temperature is 150 °C, the first curing layer starts to cure notably after being heated for ~30 min, while it only takes few minutes when the temperature is 250 °C. However, this does not suggest that a higher re-polymerization temperature is preferred during practical applications. An excessively high temperature will lead to two major pitfalls: First, it will result in shape distortion and impair the quality of the manufactured thermoset product. As shown in Fig. 8a, when the re-polymerization temperature is 250 °C, the peak residual stress in the first layer is ~0.15 MPa. This will likely lead to the fracture of the top surface due to the low strength at temperatures highly above the network T_g , or it will lead to the debonding of the top curing layer from the mold. Due to its higher stiffness, surface wrinkling may be formed as its volume shrinking. These are practical issues we observed in our experiments. Second, the rapid curing of the top layer forms a condensed film on the surface of the system, which will greatly suppress the solvent transportation, thereby slowing down the polymerization of the layers beneath it. As shown in Fig. 8b, as increasing the temperature, the curing speed of the first layer is promoted. However, its blocking effect, which is represented by the difference of subsequent layers in curing speed, tends to be more notable at high temperatures. This will lead to a significant delay in the overall curing speed of bulk epoxy, and consequently, increase the usage of electrical energy for heating and the cost of thermoset recycling.

To further reveal the influences of temperature on the recycling speed, a full re-polymerization time parameter is defined, which is taken to be the time point when the curing degree of the bottom layer reaches 80%. It is plotted as a function of heating temperature in Fig. 9. The result shows that the full re-polymerization time first decreases and then increases with the temperature. It reaches the lowest value when the temperature is ~205 °C, which is corresponding to the highest recycling speed for the epoxy samples. When the temperature is lower than 205 °C, increasing the temperature can reduce the overall re-polymerization time and promote the recycling speed due to the increased evaporation rate of the solvent and the BER rate for the chain segment connection [55,56]. Above 205 °C, although the temperature can still increase the rate of BER, the quickly formed stiff film on the solution surface starts to suppress the evaporation of EG, which in turn inhibits the re-polymerization of the polymer below it.

It should be noted that the optimal re-polymerization temperature revealed in Fig. 9 assumes that the thickness of the initial

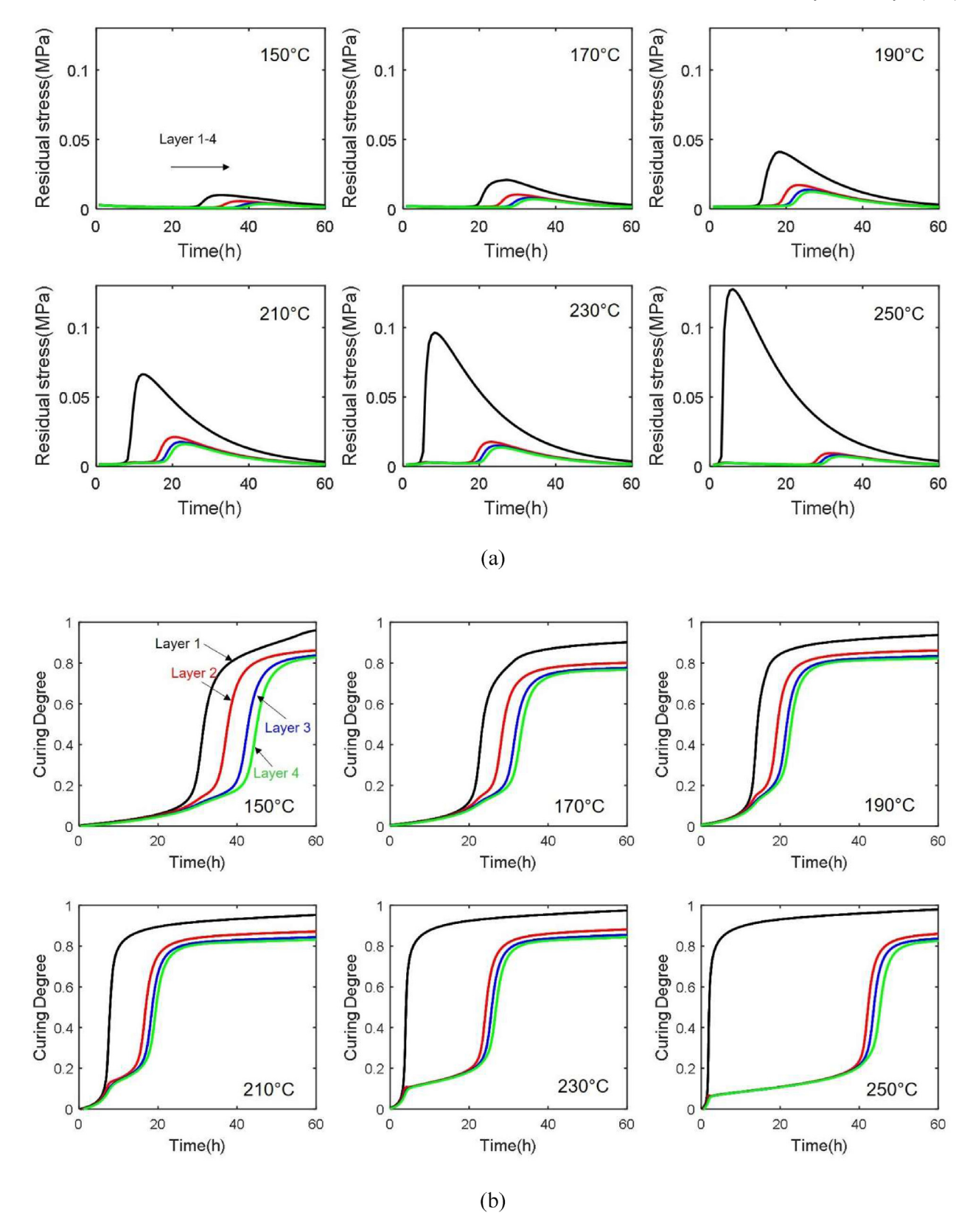


Fig. 8. (a) Predictions on the evolution of residual stress for each layer of bulk CANs at curing temperature range from 150 $^{\circ}$ C to 250 $^{\circ}$ C. (b) Predictions on the degree of repolymerization of each layer of thick CANs as function of time at curing temperature range from 150 $^{\circ}$ C to 250 $^{\circ}$ C.

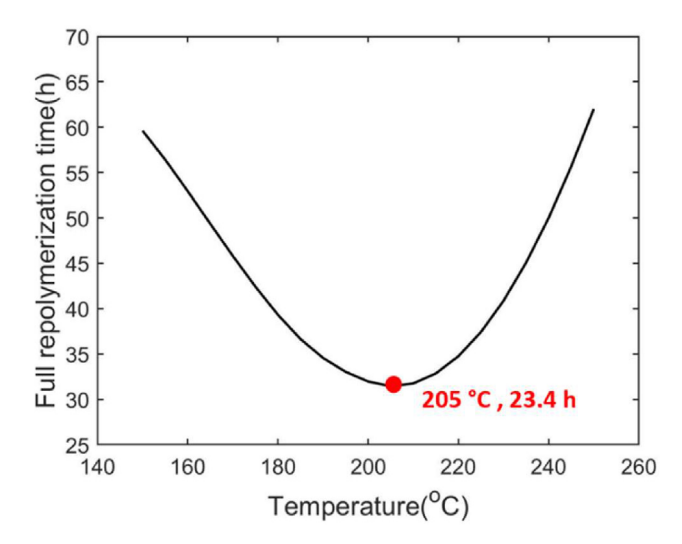


Fig. 9. The full re-polymerization time of the epoxy sample as a function of heating temperature.

polymer solution is 20 mm, and the thickness of the fully polymerized epoxy sample is \sim 7 mm. In addition, the content of the BER catalyst within the sample is 0.1 wt% with BER activation energy of 8.65 kJ/mol. It is intriguing to explore how the optimal repolymerization temperature will change with these two material parameters.

In the first group of predictions, the initial solution thickness is varied from 5 mm to 21 mm, while the BER activation energy is 8.65 kJ/mol for each case. The corresponding full re-polymerization time is plotted in Fig. 10a as a function of sample thickness and heating temperature. It is straightforward to observe that at a specific heating temperature, the re-polymerization time increases with the sample thickness (see the vertical dashed arrow) as more time is required to cure thicker samples. On the other hand, for a given sample thickness, the re-polymerization time is observed to first decrease and then increase (see the horizontal dashed arrow) with the increment of temperature. The optimal heating temperature with the lowest re-polymerization time changes with the sample thickness. For example, Fig. 10b plots the re-polymerization time as a function of heating temperature. The thickness of the initial polymer solution is 15 mm, 17 mm, 19 mm, and 21 mm, respectively. It is seen that the optimal temperature shifts toward

the lower temperature as the thickness of the material increases. This suggests that for a thicker epoxy polymer solution, a relatively lower heating temperature is preferred to fully polymerize the network with the highest speed.

In the second group of predictions, the BER activation energy is set to increase from 7.65 kI/mol to 13.15 kI/mol to represent the decreasing catalyst content. The initial thickness of the polymer solution is 20 mm in each case. The full re-polymerization time is plotted in Fig. 11a as a function of activation energy and heating temperature. The variation of the re-polymerization time shows distinguishing features compared to that with different sample thicknesses. At a relatively low temperature, e.g., 180 °C, epoxy sample with lower catalyst content (higher activation energy) reguires more time to re-polymerize due to the slower BERs (see the vertical dashed arrow at 180 °C). Therefore, the overall recycling speed is lower. However, at a relatively high temperature, e.g., 230 °C, epoxy samples with a lower catalyst content are shown to polymerize more quickly (see the vertical dashed arrow at 230 °C). This is because that the curing speed of the top surface is slower, which encourages solvent transportation and evaporations, and promotes the overall sample re-polymerization speed. This comparison suggests that as the increment of the re-polymerization temperature, the limiting factor for the overall recycling speed is changed from the lower BER rate to the blocking effect of the surface curing laver.

On the other hand, for a specific catalyst content, the repolymerization time first decreases and then increases with the temperature (see the horizontal dashed arrow). The repolymerization time with 8.7 kJ/mol, 9.2 kJ/mol, 10.2 kJ/mol, 11.2 kJ/mol, 12.2 kJ/mol, and 13.2 kJ/mol activation energy is plotted as a function of heating temperature in Fig. 11b. It is shown that a lower activation energy is corresponding to a lower optimal temperature. Therefore, for the epoxy sample with a higher catalyst content, one may need to consider using a relatively lower temperature to promote the recycling speed.

4.5. Evolution of residual stress during the manufacturing of composites with particles

The developed modeling framework is extended to study the manufacturing of particle-reinforced composites using the depolymerized solution. Specifically, the stress distribution evolution within the matrix during the re-polymerization process is investigated. Previously, Goodier [57,58] developed analytical solutions

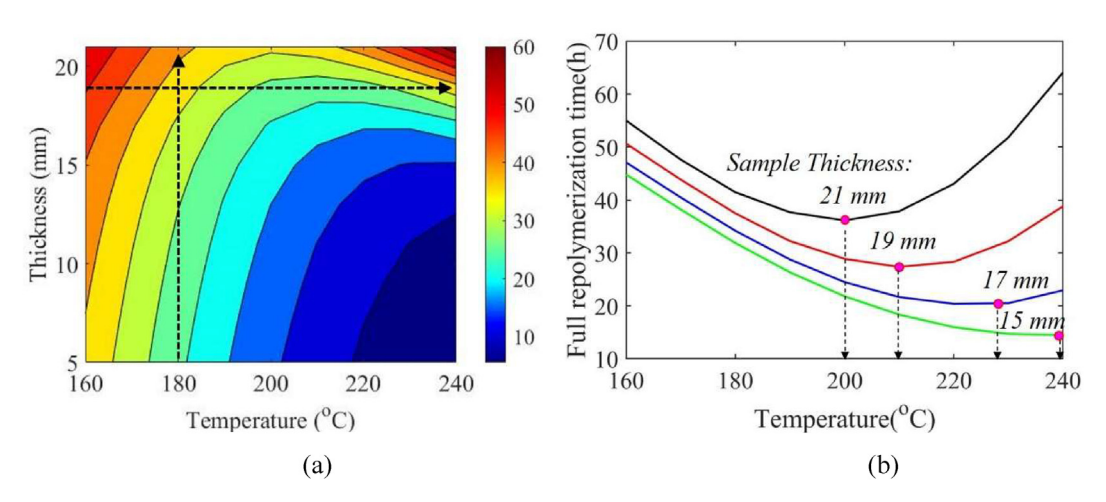


Fig. 10. (a) The full re-polymerization time of epoxy sample with different sample thickness and heating temperature. (b) The full re-polymerization time as a function of temperature.

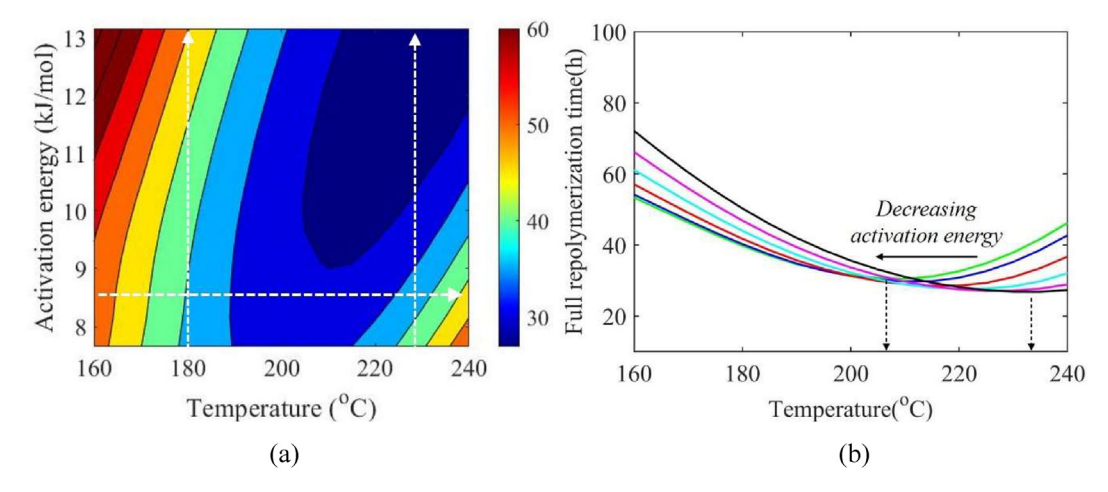


Fig. 11. (a) The full re-polymerization time of epoxy sample with different BER activation energy and heating temperature. (b) The full re-polymerization time as a function of temperature.

of the stress field around the spherical inclusions when the composite is under the simple-tension loading condition. The radial stress (σ_{rr}) and circumferential stress $(\sigma_{\theta\theta})$ around the inclusion are given by:

$$\sigma_{rr} = 2E_{eq}\left(x, t\right) \left[\frac{2A}{r^3} - \frac{2\nu}{1 - 2\nu} \frac{C}{r^3} + 12\frac{B}{r^5} + \left(-\frac{2(5 - \nu)}{1 - 2\nu} \frac{C}{r^3} + 36\frac{B}{r^5}\right) \cos 2\theta\right] + \sigma_r\left(x, t\right) \cos^2\theta, \quad (11a)$$

$$\sigma_{\theta\theta} = 2E_{eq}(x,t) \left[-\frac{2A}{r^3} - \frac{2\nu}{1 - 2\nu} \frac{C}{r^3} - 3\frac{B}{r^5} + \left(\frac{C}{r^3} - 21\frac{B}{r^5}\right) \cos 2\theta \right] + \sigma_r(x,t) \sin^2\theta,$$
(11b)

with

$$A = \frac{r_0^3 \sigma_r(x,t)}{8E_{eq}(x,t)} \frac{13 - 10\nu}{7 - 5\nu}, B = \frac{r_0^5 \sigma_r(x,t)}{8E_{eq}(x,t)} \frac{1}{7 - 5\nu}, \text{ and}$$

$$C = \frac{r_0^3 \sigma_r(x,t)}{8E_{eq}(x,t)} \frac{1}{8 - 10\nu}.$$
(11c)

In the above equations, r is the radial distance from the material point to the particle center, and r_0 is the particle radius. v is Poisson's ratio of the matrix material. During the re-polymerization process, the incompressible liquid mixture of reactive resins

gradually translates into a solid. Poisson's ratio of the final epoxy sample might be different from the initial liquid resin. However, in this study, a soft epoxy network (T_g ~30 °C) is adopted as the material platform, and the re-polymerization temperatures are highly above its glass transition temperature. The network will be in the rubbery state with a comparable Poisson's ratio as a soft rubber, which is commonly taken as a near-incompressible solid in most previous studies. Therefore, a constant Poisson's ratio is assumed in this study for the convenience of analysis. Detailed evolution of Poisson's ratio and its influences on the residual stress development deserve future rigorous study. The matrix modulus increases with time during the re-polymerization, and it is taken to be the network equilibrium modulus, $E_{eq}(x,t)$, formulated in Eq. (4). The far-field stress applied to stretch the composite is taken to be the residual stress, $\sigma_r(x,t)$, which is formulated in the Eq. (11).

It should be noted that the adopted analytical solution simplifies the problem to some extent. For example, it assumes perfect bonding between particle and matrix, but when fabricate composites using the depolymerized solution, the matrix transforms from viscous resin to a solid with considerable volume shrinkage. Therefore, the slippage between the particle and matrix may affect the stress distribution. While in our future work, finite element simulations should be performed for a more rigorous study; the analytical solution adopted in this pilot study can provide valuable and easily accessible stress analysis.

Herein, a cubic representative element with a side length of 20 mm is created, and a spherical particle (1 mm diameter) is

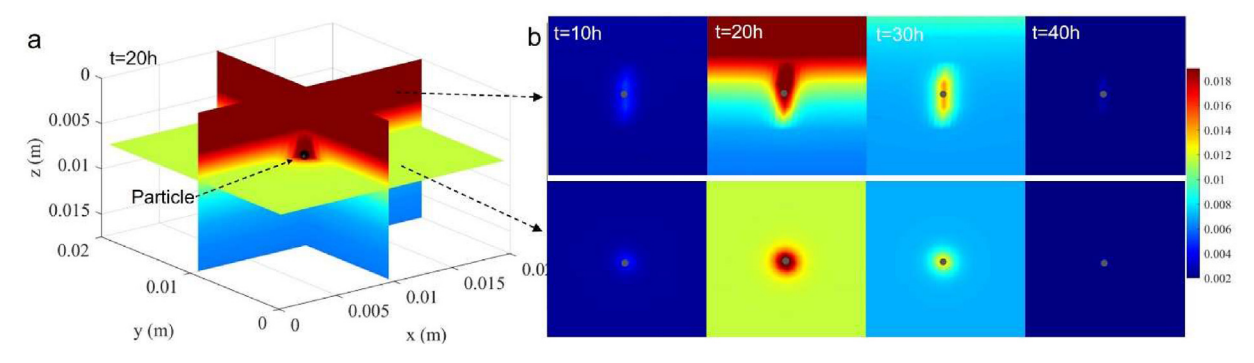


Fig. 12. (a) 3D view of the distribution of stress during the re-polymerization of the composite with particle reinforcement. The system has been heated at 180 °C for 20 h. (b) The distribution of stress on a vertical plane and horizontal plane that both pass through the particle. The heating time is 10 h, 20 h, 30 h, and 40 h, respectively at 180 °C.

placed in the volume center. The solvent evaporation boundary condition is applied on the top surface. The volume element is sliced into 20 layers parallel to the top surface. Using the developed modeling framework, the evolution of the network equilibrium modulus and residual stress development in each layer can be predicted, which are submitted into Eq. (11) to calculate the stress components, which are integrated into the von Mises stress to characterize the stress distribution.

Fig. 12a shows the stress distribution on three cross-sectional planes of the volume element that pass through the particles, which gives a 3D view of the stress distribution within the matrix. The volume element is heated at 180 °C for 20 h. Fig. 12b shows the evolution of the stress field on the vertical and horizontal crosssectional planes with different heating times. It is observed that on the horizontal cross-sectional plane, notable stress concentration exists around the particle. The stress contour is circular because the curing layer is in the equibiaxial tension state. When it is away from the particle, the stress distribution within the matrix is relatively uniform. In contrast, the stress distribution on the vertical planes is highly nonuniform because each horizontal layer has different degrees of volume shrinkage and stress. In addition to the stress concentration around the particle, a high stress amplitude exhibits on the top surface due to the rapid solvent evaporation and re-polymerization. Note that the highest stress still exists around the particle on the vertical cross-sectional plane. For example, after being heated for 20 h, the stress on the top and the highest stress around the particle are ~0.14 MPa and ~0.18 MPa, respectively. With the increment of heating time, both stress in the matrix and stress concentration around the particle first increase due to the volume shrinkage of the matrix and then decrease due to the BER-induced stress relaxation. After being heated for 40 h, the epoxy matrix is fully polymerized, and the amplitude of residual stress approaches zero within the system.

The significant stress concentration developed around the particle during the manufacturing of composites is risky as it may lead to the debonding between the particles and matrix, as well as the fracture of the epoxy matrix around the particle. The open microcracks cannot be automatically healed, which compromises the mechanical strength of the fabricated composites. In Fig. 13, the maximum residual stress around the particle is predicted as a function of heating time at different temperatures. It is observed that the highest stress increases with the temperature. When the temperature is 190 °C, the peak stress is ~0.22 MPa. Considering the

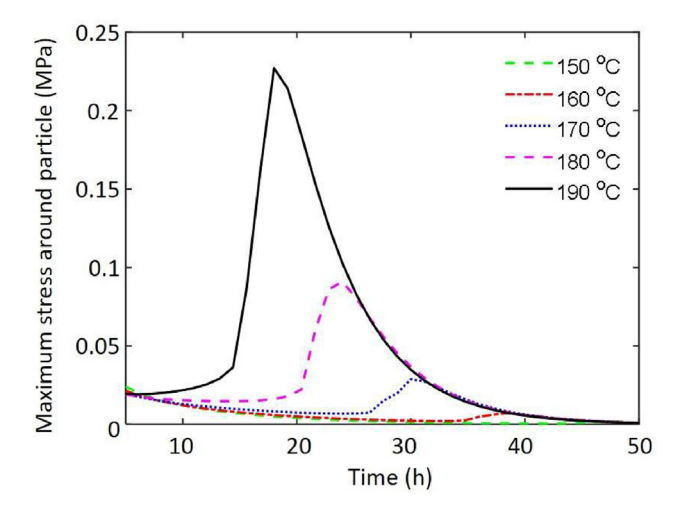


Fig. 13. The evolution of the maximum stress around the particle as a function of heating time during the re-polymerization of the composite.

evolution of the equilibrium modulus during the network repolymerization (0.5 MPa–2.5 MPa), the stress amplitude can generate a ~9% principal strain at least. Since the re-polymerization temperature is highly above the network T_g (~30 °C), the network tends to be brittle, and the residual stress is likely to lead to material failure. Decreasing the temperature reduces the peak stress amplitude and the risk for particle debonding, but the trade-off is the overall manufacturing speed. Therefore, during the practical applications, a temperature 'sweet spot' can be identified using the developed modeling framework to enable both high quality and low manufacturing cost of the composites.

5. Conclusion

When recycling thermoset wastes using organic solvents, the solvent evaporation during the re-polymerization step leads to notable volume shrinkage of the resin and residual stress development. The reaction starts from the surface, leading to nonuniform material properties and curing degree in the sample thickness direction. In this work, the evolution of the stress field and material properties during the solvent-assisted recycling of thermosetting polymers is studied. The influences of heating temperature are experimentally examined. It shows that a higher temperature promotes the reaction and re-polymerization rates, which leads to a higher stress field within the network. A solidified thin film can be quickly formed on the top surface of the resin, which suppresses the curing of the network beneath it. A diffusion-reaction-kinetic modeling framework is developed to assist the study, which links the microscale reaction kinetics of chain connection and cleavage to the macroscale volume shrinkage and material mechanical properties. The modeling framework is shown to precisely capture the experimental observations. It is applied to examine the influences of the temperature, sample thickness, and content of the BER catalyst. It shows that for a sample with a higher thickness or a higher content of the BER catalyst, a relatively low temperature is preferred to increase the overall recycling speed. The modeling framework is extended to study the recycling of composite with particle reinforcements. The stress concentration around the particles during the composite manufacturing may lead to the debonding between particle and epoxy matrix. It can be substantially mitigated using lower processing temperatures, which improve the quality and mechanical performance of the fabricated composites. Overall, this study reveals the relationship between re-polymerization degree and the residual stress development during the solvent-assisted recycling of thermoset wastes, which provides a guideline to design material and processing conditions to promote the recycling speed, reduce the recycling cost, and improve the quality and mechanical properties of recycled thermosets.

Authorship statement

Xiaojuan Shi: Conceptualization, Methodology, Visualization, Writing — original draft. **Drake Soule:** Methodology, Investigation, Visualization, Writing — original draft. **Qi Ge:** Validation, Writing — review and editing. **Haibao Lu:** Validation, Writing — review and editing. **Kai Yu:** Conceptualization, Writing — review and editing, Supervision, Project administration, Funding acquisition.

Declaration of competing interest

The authors declare that they have no known competing financial interests or personal relationships that could have appeared to influence the work reported in this paper.

Acknowledgments

K.Y. acknowledges support from the National Science Foundation (grant CMMI-1901807), USA.

Appendix A. Supplementary data

Supplementary data to this article can be found online at https://doi.org/10.1016/j.mtsust.2022.100167.

References

- D. Bower, Morphology and Motion, an Introduction to Polymer Physics, Cambridge University Press, Cambridge, 2002, pp. 133–137, 2002.
- [2] G.N. Hartt, D.P. Carey, Economics of Recycling Thermosets, SAE Technical Paper 920802, Society of Automobile Engineers, Warrendale, PA, 1992.
- [3] C.E. Kouparitsas, et al., Recycling of the fibrous fraction of reinforced thermoset composites, Polym. Compos. 23 (2002) 682–689.
- [4] K. Ogi, et al., Mechanical properties of abs resin reinforced with recycled cfrp, Adv. Compos. Mater. 16 (2007) 181–194.
- [5] S.J. Pickering, Recycling technologies for thermoset composite materials current status, Compos. Appl. Sci. Manuf. 37 (2006) 1206–1215.
- [6] J. Palmer, et al., Successful closed-loop recycling of thermoset composites, Compos. Appl. Sci. Manuf. 40 (2009) 490–498.
- [7] A. Conroy, et al., Composite recycling in the construction industry, Compos. Appl. Sci. Manuf. 37 (2006) 1216–1222.
- [8] P.T. Williams, et al., Recovery of value-added products from the pyrolytic recycling of glass-fibre-reinforced composite plastic waste, J. Energy Inst. 78 (2005) 51–61.
- [9] R.E. Allred, Recycling process for scrap composites and prepregs, SAMPE J. 32 (1996) 46–51.
- [10] R.E. Allred, et al., Properties of carbon fibers reclaimed from composite manufacturing scrap by tertiary recycling, Technology Transfer in a Global Community 28 (1996) 139–150.
- [11] R.E. Allred, et al., Recycling process for carbon/epoxy composites, 2001, A Materials and Processes Odyssey 46 (2001) 179–192. Books 1 and 2.
- [12] G. Jiang, et al., Soft ionisation analysis of evolved gas for oxidative decomposition of an epoxy resin/carbon fibre composite, Thermochim. Acta 454 (2007) 109–115.
- [13] H.L.H. Yip, et al., Characterisation of carbon fibres recycled from scrap composites using fluidised bed process, Plastics Rubber and Composites 31 (2002) 278–282.
- [14] B.J. Jody, et al., A process to recover carbon fibres from polymer matrix composite scrap, Int SAMPE Symp Exhibition 49 (2004) 35–47.
- [15] T. Liu, et al., Mild chemical recycling of aerospace fiber/epoxy composite wastes and utilization of the decomposed resin, Polym. Degrad. Stabil. 139 (2017) 20–27.
- [16] A.D. La Rosa, et al., Recycling treatment of carbon fibre/epoxy composites: materials recovery and characterization and environmental impacts through life cycle assessment, Compos. B Eng. 104 (2016) 17–25.
- [17] S. Ma, D.C. Webster, Degradable thermosets based on labile bonds or linkages: a review, Prog. Polym. Sci. 76 (2018) 65–110.
- [18] C.J. Kloxin, et al., Covalent adaptable networks (cans): a unique paradigm in cross-linked polymers, Macromolecules 43 (2010) 2643–2653.
- [19] C.N. Bowman, C.J. Kloxin, Covalent adaptable networks: reversible bond structures incorporated in polymer networks, Angew. Chem. Int. Ed. 51 (2012) 4272–4274.
- [20] K. Yu, et al., Interfacial welding of dynamic covalent network polymers, J. Mech. Phys. Solid. 94 (2016) 1–17.
- [21] B.J. Adzima, et al., Rheological and chemical analysis of reverse gelation in a covalently cross-linked diels-alder polymer network, Macromolecules 41 (2008) 9112–9117.
- [22] M.A. Tasdelen, Diels—alder "click" reactions: recent applications in polymer and material science, Polym. Chem. 2 (2011) 2133—2145.
- [23] R.J. Wojtecki, et al., Using the dynamic bond to access macroscopically responsive structurally dynamic polymers, Nat. Mater. 10 (2011) 14–27.
- [24] X. Shi, et al., The nonequilibrium behaviors of covalent adaptable network polymers during the topology transition, Soft Matter 17 (2021) 2104–2119.
- [25] C. Luo, et al., Effects of bond exchange reactions and relaxation of polymer chains on the thermomechanical behaviors of covalent adaptable network polymers, Polymer 153 (2018) 43–51.
- [26] D.W. Hanzon, et al., Adaptable liquid crystal elastomers with transesterification-based bond exchange reactions, Soft Matter 14 (2018) 951–960.

- [27] X. He, et al., Cyclic welding behavior of covalent adaptable network polymers, J. Polym. Sci. B Polym. Phys. 56 (2018) 402–413.
- [28] D.W. Hanzon, et al., Creep-induced anisotropy in covalent adaptable network polymers, Soft Matter 13 (2017) 7061–7073.
- [29] K. Yu, et al., A computational model for surface welding in covalent adaptable networks using finite-element analysis, Journal of Applied Mechanics-Transactions of the ASME 83 (2016) 91002—91013.
- [30] K. Yu, et al., Carbon fiber reinforced thermoset composite with near 100% recyclability, Adv. Funct. Mater. 26 (2016) 6098–6106.
- [31] Q. Shi, et al., Solvent assisted pressure-free surface welding and reprocessing of malleable epoxy polymers, Macromolecules 49 (2016) 5527–5537.
- [32] X. He, et al., Primary recycling of anhydride-cured engineering epoxy using alcohol solvent, 3D Print. Addit. Manuf. 6 (2019) 31–39.
- [33] K. Yu, et al., Dissolution of covalent adaptable network polymers in organic solvent, J. Mech. Phys. Solid. 109 (2017) 78–94.
- [34] Q. Shi, et al., Recyclable 3d printing of vitrimer epoxy, Mater. Horiz. 4 (2017) 598–607.
- [35] X. Shi, et al., Interfacial welding and reprocessing of engineering thermosets based on surface depolymerization, Surface. Interfac. 26 (2021) 101368.
- [36] L.M. Johnson, et al., Controlled degradation of disulfide-based epoxy thermosets for extreme environments, Polymer 64 (2015) 84–92.
- [37] A.R. Luzuriaga, et al., Epoxy resin with exchangeable disulfide crosslinks to obtain reprocessable, repairable and recyclable fiber-reinforced thermoset composites, Mater. Horiz. 3 (2016) 241–247.
- [38] P. Taynton, et al., Repairable woven carbon fiber composites with full recyclability enabled by malleable polyimine networks, Adv. Mater. 28 (2016) 2904–2909
- [39] X. He, et al., Recyclable 3d printing of polyimine-based covalent adaptable network polymers, 3D Print. Addit. Manuf. 6 (2019) 31–39.
- [40] X. He, et al., Reshapeable, rehealable and recyclable sensor fabricated by direct ink writing of conductive composites based on covalent adaptable network polymers, International Journal of Extreme Manufacturing 4 (2021), 015301.
- [41] X. He, et al., A sustainable manufacturing method of thermoset composites based on covalent adaptable network polymers, Compos. B Eng. 221 (2021) 109004
- [42] X. He, et al., 3d printing of continuous fiber-reinforced thermoset composites, Addit. Manuf. 40 (2021) 101921.
- [43] P. Taynton, et al., Heat-or water-driven malleability in a highly recyclable covalent network polymer, Adv. Mater. 26 (2014) 3938–3942.
- [44] X. Shi, et al., A multiscale chemomechanics theory for the solvent—assisted recycling of covalent adaptable network polymers, J. Mech. Phys. Solid. (2020) 103918
- [45] D. Montarnal, et al., Silica-like malleable materials from permanent organic networks, Science 334 (2011) 965–968.
- [46] V.V. Krongauz, Diffusion in polymers dependence on crosslink density, J. Therm. Anal. Calorim. 102 (2010) 435–445.
- [47] S. Gan, et al., A viscoelastic description of the glass transition-conversion relationship for reactive polymers, J. Therm. Anal. 37 (1991) 463–478.
- [48] A. DiBenedetto, Prediction of the glass transition temperature of polymers: a model based on the principle of corresponding states, J. Polym. Sci. B Polym. Phys. 25 (1987) 1949–1969.
- [49] L.E. Nielsen, Cross-linking—effect on physical properties of polymers, J. Macromol. Sci., Part C. 3 (1969) 69–103.
- [50] M. Dewaele, et al., Volume contraction in photocured dental resins: the shrinkage-conversion relationship revisited, Dent. Mater. 22 (2006) 359–365.
- [51] K. Yu, et al., Reprocessing and Recycling of Thermoset Polymers Based on Bond Exchange Reaction, 2014.
- [52] K. Yu, et al., Influence of stoichiometry on the glass transition and bond exchange reactions in epoxy thermoset polymers, RSC Adv. 4 (2014) 48682–48690.
- [53] C. Luo, et al., Chemomechanics in the moisture-induced malleability of polyimine-based covalent adaptable networks, Macromolecules 51 (2018) 9825–9838.
- [54] C. Luo, et al., Chemomechanics of dual-stage reprocessable thermosets, J. Mech. Phys. Solid. 126 (2019) 168–186.
- [55] B. Zhang, et al., Influences of processing conditions on mechanical properties of recycled epoxy-anhydride vitrimers, J. Appl. Polym. Sci. (2020) 49246.
- [56] H. Li, et al., Influence of treating parameters on thermomechanical properties of recycled epoxy-acid vitrimers, Soft Matter 16 (2020) 1668–1677.
- [57] J.N. Goodier, Concentration of stress around spherical and cylindrical inclusions and flaws, Trans. ASME. 55 (1933) 39–44.
- [58] Y. Fukahori, W. Seki, Stress analysis of elastomeric materials at large extensions using the finite element method, J. Mater. Sci. 28 (1993) 4471–4482.